

Computational hemodynamics in a patient - specific cerebral aneurysms models

S. Gaivas¹, P. Cârlescu², Ion Poată³

¹PhD student, “Gr.T.Popa” UMPH, Iași, Romania

²“Ion Ionescu de la Brad” University of Agriculture Science and Veterinary Medicine, Iași

³“Gr.T. Popa” UMPH Iasi

Abstract

Backgrounds: Hemodynamic factors are known to play an important role in initiation, growth and rupture of intracerebral aneurysms. Thorough knowledge of hemodynamic parameters in cerebral arteries and aneurysms are very useful in understanding of pathophysiology and clinical evaluation of cerebral aneurysms. We describe a methodology of computational analysis of hemodynamics in a patient specific aneurysms models. Aneurysms are segmented from CT angiography images.

Method: A total of 6 cerebral aneurysms models were developed from CT angiography images. A computational fluid dynamics analyses were accomplished under realistic flow conditions. We selected only patients with multiple intracerebral aneurysms and conducted hemodynamic studies in un-ruptured aneurysms. We tried to evaluate the rupture risks for these aneurysms. In our series were five middle cerebral artery aneurysm and one basilar artery aneurysm.

Results: We succeed to set up a methodology in patient specific aneurysms models hemodynamic study. Computational analyses of hemodynamic factors were performed for each of these 6

aneurysms models. The results were then processed to determine the average pressure on the arterial wall and inside the aneurysm, stream lines and region of greater impact of hemodynamic forces.

Conclusions: Wall shear stress plays an important role in initiation, growth and rupture of cerebral aneurysms. In vivo measurements of WSS values had become most popularly in last decade. Aneurysm geometry influences the characteristics of flow conditions.

Keywords: Computational fluid dynamics, aneurysm geometry, Wall shear stress.

Introduction

Hemodynamics is the study of physical forces involved in blood circulation and namely hemodynamics refers to physical factors governing the flow of blood in circulatory system. Hemodynamic parameters are considered to be responsible for initiating, growth and rupture of cerebral aneurysms. Hemodynamic factors play a vital role in regulating the structure and function of the endothelial layer. Endothelial cell capacity to respond to shear forces is responsible for structural remodeling of the entire vessel lumen diameter (3, 11). This morphological

variation of vascular endothelial cells results in different degrees of vasoactive substances productions, such as nitric oxide (ON) (5, 4, 10). A uniform shear force tends to shape and align endothelial cells in the direction of flow, while a low shear force, in a hemodynamically oscillator environment, causes an irregular shape and lack of specific orientation. In addition, a small shear stress changes the phenotype of endothelial cells from atheroprotection to atherogenesis with an increased rate of cell turnover. Increased arterial blood flow produce adaptive response of arterial wall histology, leading to an increase in vessel diameter and a reduction of shear forces to basic physiological values. However, if the forces are high in one place they can cause a focal enlargement and a widening of arterial wall, process called destructive modeling, which is induced by an excessive production of molecules, such as nitric oxide (ON). The flow dynamics have been studied in a multitude experimental models to better understand their role in aneurysms behavior. Patients specific aneurysms geometry study of hemodynamic forces have been accomplished by several authors in last decade. (2, 7, 8). The aim of all these studies is to find the correlation between the geometry of aneurysms and flow pattern. The purpose of our study were to demonstrate the feasibility of development of computational analyses of wall shear stress in cerebral aneurysms from CT angiography images in our Hospital.

Methods

Data acquisition on the 3D geometry of an aneurysm was achieved, in the first stage by performing CT angiography. CT angiography exploration was done using a

CT scanner device Aura 2001 Philips Medical Systems (Tube Counts: 273.000, Gantry Counts: 1,030,018; Workstation: Sun Ultra 10, MRC 162, 3.5 MHU, Software Upgrade in 2006, DICOM, options: Bone, 3D, CTA, Rapid View Reconstruction). Image acquisition protocol was achieved by setting following radiographic parameters: maximum allowed tube power 120 kV, 150mA, 15 cm field of view, 1-2 mm collimators with 1:1 pitch and at 0.7 to 1 mm reconstruction intercalation of 0.5-1 mm range. A total of 100 ml contrast agent (300 mg iodine / ml) was injected intravenously in a brachial vein with a self-acting injector at a rate of injection of 2.5 ml / sec. Image acquisition is triggered with a delay of 14 seconds from the time of injection of the contrast. In this way were obtained a number of 90-120 axial images in DICOM format with extension. dcm.

Assembly of these images (*. dcm) and contour transformation of the 2D plane images in a 3D volume was performed with the software AVIZO v6.3. Figure 1.

AVIZO software is used to extract an area of interest as follows:

1. Defining the region of interest (ROI)
2. Vascular surface extraction (aneurysm sought) of the 3D image obtained from CT angiography
3. Surfacing by rendering using a bright field of voxel intensity between 90 and 130. Establish the precise amount is achieved by trial and error method according to the obtained image quality and dimensional accuracy of the vessels.
4. using isosurface command Applied to surface is obtained triangulation (obtaining a number of interconnected triangles) and save it as surface triangles in stereolithography format (stl).

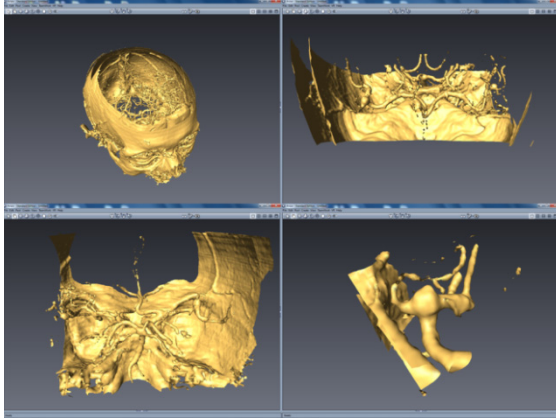


Figure 1 3D volume of cerebral arteries seen in AVIZO software programme

.Stl file extension obtained in AVIZO is imported in CAD software program (Computer Aided Design) SolidWorks 2011 where is processed by removing additional basic areas file without aneurysm geometry changes. These processing are designed to check the quality of the obtained geometry and optimization of file size, saved in ASCII format with the extension (.sat). This method of reconstruction is the most precise and operator influence on final geometry is minimal (Figure 2).

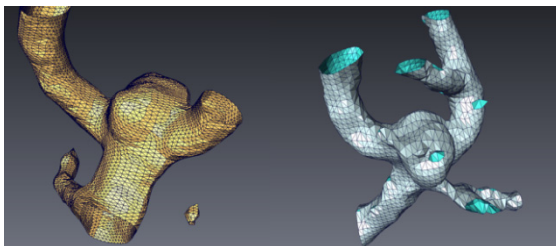


Figure 2 meshing generation

File obtained in Gambit is imported in software program FLUENT v.6.3.26 (ANSYS. Inc.) and processed by preprocessing, processing and postprocessing.

Preprocessing

- Workload dimensional calibration.

- The quality meshing check.

- Introduction of blood parameters

Blood is considered a Newtonian fluid with density $\rho = 1050$ [kg/m³] and dynamic viscosity $\eta = 0.004$ [kg / m • s] (Poiseuille)

Although blood has actually non-Newtonian behavior in the simulation it is considered Newtonian because there were no significant differences in the distribution of WSS (wall shear stress) (11)

Physiological conditions of blood flow at the entrance have been imposed using the flow measurements in internal carotid artery of a normal patient. Measurements were made with a Doppler ultrasound at the heart beat rhythm of 70 beats / min.

Average blood flow speed in the artery was 0.344 [m / s] and peak systolic drop occurred at $t = 0.13$ [s]. Time dependence of the mean flow velocity was represented by following 10 factors: $a=2559,3$; $b=10450$; $c=19138$; $d=20959$; $e=15174$; $f=7391,9$; $g = 2320,6$; $h = 418,15$; $i = 30,93$; $j = 0,693$; $k = 0,191$.

$$V_{\max} = a \cdot t^{10} - b \cdot t^9 + c \cdot t^8 - d \cdot t^7 + e \cdot t^6 - f \cdot t^5 + g \cdot t^4 - h \cdot t^3 + i \cdot t^2 \cdot j \cdot t + k \quad (1)$$

where: t - systole-diastole complete cycle (between 0-0.75[s]). Given that the artery is approximately circular, velocity distribution is considered parabolic in the artery entry, with a maximum into a center of the vessel and a minimum close to the vessel wall. Complete equation of speed input section is:

$$V_{(t,r)} = \left(V_{\max} \cdot \left(1 - \frac{z^2 + y^2}{r^2} \right) \right) \quad (2)$$

where:

r - inner radius of the vessel in the input,
 y and z - coordinates in the plane of entry.

Velocity equation V is introduced as a function UDF (User Defined Function) written in C++ programming language. Womersley number is a dimensionless number used in fluid mechanics.

The Womersley number is also important in determining the boundary layer thickness formed at the vessel wall, while noting that the end effect can be ignored.

Womersley number (α) depends on: flow rate, model geometry and Newtonian fluid viscosity and varies with vessel diameter at the entrance to each case. Womersley number equation is:

$$\alpha = r \cdot \sqrt{\frac{2 \cdot \pi \cdot v \cdot \rho}{\eta}} \quad (3)$$

where:

r [m]-entry of the vessel radius, v [1 / s] - flow rate, ρ [kg/m³] - blood density, η [kg / m • s] - blood viscosity. Exact solution given by Womersley may be used to input, since α (small values) is very close to the solution for velocity function $V(t, r)$.

Flow regime is given by the dimensionless Reynolds number (Re). This number varies with the diameter of the vessel for each case.

$$Re = \frac{\rho \cdot V \cdot d}{\eta} \quad (4)$$

where: ρ [kg/m³] - blood density, V [m / s] - maximum speed of blood flow at the entrance, d [m] - diameter at the entrance of the vessel, η [kg/m•s]-blood viscosity. Depending on this number blood flow values in the model can be:

- Laminar when $Re \leq 2300$,
- Transient time $2300 < Re < 10000$,
- Turbulent when $Re > 10000$.

The Reynolds number and Womersley number governs the dynamic similarity.

Processing

Governing equations were solved in FLUENT which use finite volume method for spatial discretization conducted in Gambit. Equations of momentum and mass conservation for incompressible fluid can be written as:

$$\nabla \cdot V = 0 \quad (5)$$

$$\rho \cdot \left(\frac{\partial V}{\partial t} + V \cdot \nabla V \right) = -\nabla p + \nabla \cdot \tau \quad (6)$$

where: $\nabla = \frac{\partial}{\partial x} + \frac{\partial}{\partial y} + \frac{\partial}{\partial z}$ - Laplace operator,

ρ - density of blood, V -velocity field, p - pressure, τ - pressure tensor. Speed and pressure

interpolations were based on power law and second order respectively. Pressure coupling was obtained using speed SIMPLEC algorithm. (Semi-Default Method for Pressure-Linked equations consistency) (5) If flow is laminar, Wall Shear Stress is defined as the velocity gradient at the wall, through the relation:

$$\tau_w = \eta \cdot \frac{\partial V}{\partial n} \quad (7)$$

where τ_w [Pa] - tension tangential to the wall, η [kg / m • s] - blood viscosity, V [m / s] - the speed of blood flow in the vessel wall considered, N - normal direction to the vessel wall. The condition for the default time was conducted marking the second order scheme, with a time step $\Delta t = 0.001$ [s]. It was also used for calculating the maximum number of iterations for a time step of 5. The total time of calculation was 0.75 [s]. Peak systolic flow is obtained at $t = 0.13$ [s] and time averaged Reynolds number is denoted by Rem. The systolic peak flow Reynolds number is denoted by $Re = Re_{max}$ in the table (see Table 1-3). This number is lower than 2300, so that input can be considered as laminar flow.

Postprocessing

In postprocessing WSS values are in [N/m²] = [Pa], 1 N/m² = 0.0075 mm Hg; speed V [m / s].

Results

Computational models of 6 intracranial aneurysms have been constructed from CT angiography images. Two of six aneurysm 3D reconstructed images are shown in figure 3. After reconstruction and meshing of corresponding anatomical aneurysms images CFD simulation analysis were performed for each of the six aneurysm. Average values of WSS are calculated throughout the cardiac cycle, but we present maximum values of WSS at 0.13 sec (peak systolic) and at 0.6 sec (peak diastolic). The results of maximum wall shear stress at peak systolic and diastolic flow and the site of maximum wall hit are shown in table 4. Wall shear stress inside the aneurysm dome are shown in table 5.

TABLE 1

Womersley and Reynolds number values for aneurysms

aneurysm model	Womersley α	Reynolds		Conditions imposed in the CFD simulation
		Re_m	Re	
Aneurysm 1	2,074	214,987	271	Laminar flow; without boundary layer
Aneurysm 2	3,249	336,813	424	Laminar flow; without boundary layer
Aneurysm 3	2,350	243,652	307	Laminar flow; without boundary layer
Aneurysm 4	1,382	143,325	181	Laminar flow; without boundary layer
Aneurysm 5	2,212	229,320	289	Laminar flow; without boundary layer
Aneurysm 6	1,866	193,488	244	Laminar flow; without boundary layer

Reference at $t = 0.13$ resulting $V_{max} = 0.344$ [m/s], and at $t = 0.6$ resulting $V_{min} = 0.202$ [m/s].

TABLE 2

Values used for aneurysms

aneurysm model	r [m]	d [m]	ρ [Kg/m ³]	η [Kg/m·s]	V [m/s]		ν [Hz]
					$t=0,13$ [s]	$t=0,6$ [s]	
Aneurysm 1	0,0015	0,003	1050	0,004	0,344	0,202	1,16
Aneurysm 2	0,00235	0,0047	1050	0,004	0,344	0,202	1,16
Aneurysm3	0,0017	0,0034	1050	0,004	0,344	0,202	1,16
Aneurysm4	0,001	0,002	1050	0,004	0,344	0,202	1,16
Aneurysm 5	0,0016	0,0032	1050	0,004	0,344	0,202	1,16
Aneurysm 6	0,00135	0,0027	1050	0,004	0,344	0,202	1,16

TABLE 3

Number of elements and quality used for each aneurysms

aneurysm model	Number of mesh elements	Mesh quality	Mesh type
Aneurysm 1	36623	0,9	tetrahedral
Aneurysm 2	19824	0,83	tetrahedral+hexahedral
Aneurysm3	82489	0,81	tetrahedral+ hexahedral
Aneurysm4	232730	0,91	tetrahedral
Aneurysm5	100892	0,81	tetrahedral+ hexahedral
Aneurysm 6	90350	0,8	tetrahedral+ hexahedral

TABLE 4

Wall shear stress at peak systole and diastole heart beat

Aneurysm models	Time		Area of max WSS
	0,13 [s]	0,6 [s]	
	WSS [Pa]	WSS [Pa]	
Aneurysm 1	9,2	5,13	Origin of bifurcation
Aneurysm 2	17,3	10,5	Origin of bifurcation
Aneurysm 3	21,7	12,8	Origin of bifurcation
Aneurysm 4	22,3	13,5	Origin of bifurcation
Aneurysm 5	9,01	5,24	Origin of a branch
Aneurysm 6	6,16	3,68	Origin of bifurcation

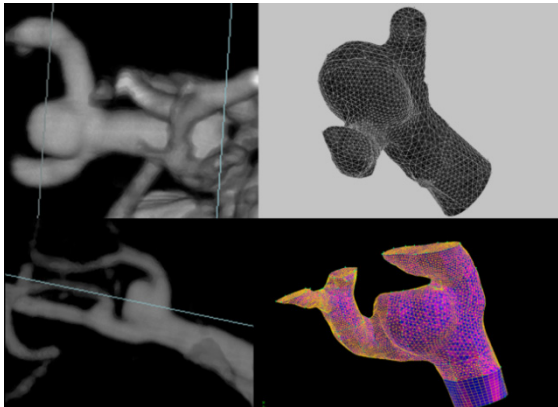


Figure 3 Reconstructed 3D aneurysms models

TABLE 5

Maximum WSS inside the aneurysms

Aneurysm models	Time	
	0,13 [s]	0,6 [s]
Aneurysm 1	0,46	0,25
Aneurysm 2	1,15	0,7
Aneurysm 3	0,7	0,42
Aneurysm 4	0,74	0,45
Aneurysm 5	0,3	0,17
Aneurysm 6	0,3	0,18

Fluid movement is viewed using the intuitive stream lines. These stream lines are representative of the speed in a given time. Intra-aneurysmal flow velocity shows a variety of model flow in aneurysms studied. Each aneurysm has its unique hemodynamic profile, but many aneurysms have the same characteristics. The most common jet inflow had maximum collision in the aneurysm neck. After impact on the wall of the aneurysms, the inflow jet disintegrate into one or more “whirlpools”, depending on the aneurysm geometry. Figure 4 shows different types of flow, represented by stream lines, and different models of whirlpools depending on the geometry of the aneurysm. Vortices inside the aneurysms differ from simple single vortices, double to chaotic vortices.

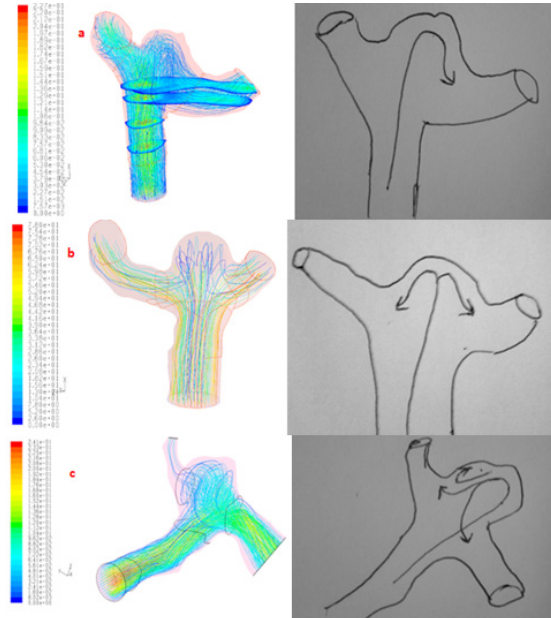


Figure 4 Different types of stream lines and whirlpools inside the aneurysm

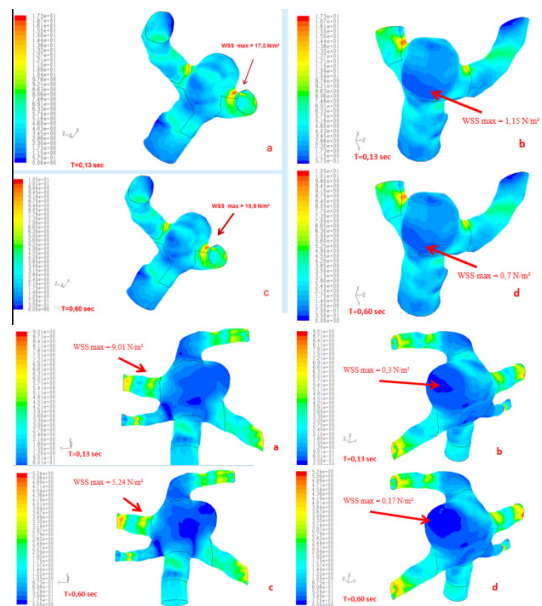


Figure 5 Two examples of aneurysms models with maximum WSS values shown

In figure 5 are shown two examples of computational simulation of WSS in aneurysms. Maximum WSS at peak systole and diastole differ in all 6 examples of our aneurysm simulation. The value vary from

6,16 N/m² to 22,3 N/m² at peak systole cardiac beat. In diastole the values are smaller, varying from 3,68 to 13,5 N/m². In all aneurysm models the maximum of WSS were at the origin of bifurcation branch see Figure 6. Inside the aneurysm the value of WSS were found to be much lower than in other parts of the segmented region.

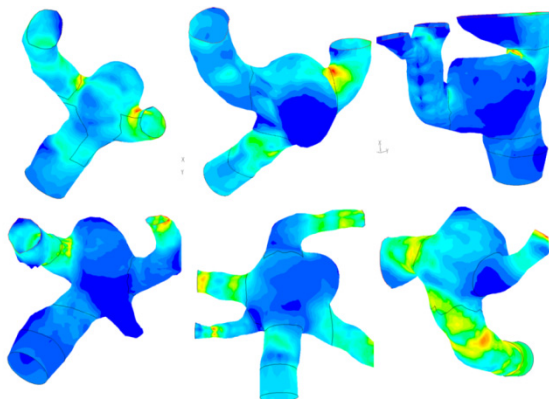


Figure 6 All 6 models of aneurysm simulation with the maximum WSS at the origin of bifurcation branch

Discussion

Computational fluid dynamics is used in many areas, especially in engineering world. This new domain provides very detailed information about fluid characteristics such as velocity, temperature, and concentration. Medical science lent this new technology to study hemodynamics within the body. In cerebral aneurysm CFD help us to understand their formation, growth, and rupture through study of aneurysm properties such as geometry, blood flow characteristics, density, viscosity and velocity. By studying of wall shear stress inside the aneurysms resulting from blood flow it becomes more clear how aneurysm has occurred. The wall shear stress (WSS), plays a major role in the growth and rupture of cerebral aneurysms. Shojima et al. (13) presented the results of statistical analysis of

the magnitude of WSS in and around aneurysms. His study shows that the magnitude of the wall shear is greatest along the aneurysmal neck, and not at the top or aneurysmal pouch. Aneurysm growth is produced at the neck level, where WSS values are higher, while aneurysm rupture occurs in the aneurysm body, where the WSS are lower. WSS acts directly on the endothelial layer, and modulates endothelial cell function (11). It was found that vascular endothelium regulates arterial wall properties through a mechanism related to blood shear forces and maintains physiological reference WSS within 15 to 20 dyn/cm². This is achieved by endothelial cells that play an important role in the regulation of pressure in the WSS-physiological limits, by initiating a process of vascular remodeling (5). In our models the higher WSS were found around the region of the aneurysm neck. Inside the aneurysm body were found very lower WSS values, which leads us to believe that low flow theory is involved in aneurysm rupture.

Conclusions

We presented a methodology for simulation of intraaneurysmal flow in patient specific models of aneurysms. Flow analysis shows that flow model is not similar for all patients. Flow characteristics are highly dependent on the geometry of the vessels and aneurysms. These techniques based on computer flow study are important for understanding the relationship between hemodynamic parameters and risk of rupture, and will be very useful since it can be done by routine clinical environment. We have developed a segmentation algorithm to work with the CT angiography images to perform CFD simulations.

References

1. Castro M.A., Putman C.M., Cebal J.R. (2005) Application of vascular CFD for clinical evaluation of cerebral aneurysms. *Computational Fluid and Solid Mechanics*.
2. Cebal, J.R., Castro, M.A., Soto, O., Lohner, R., and Alperin, N., (2003), "Blood-flow models of the circle of Willis from magnetic resonance data", *J. Eng. Math.*, 47, 369-386
3. Drexler H., Hornig B. Endothelial dysfunction in human disease. *J. Mol. Cell. Cardiol.* 1999;31:51-60. [PubMed]
4. Ferziger JH, Peric M. *Computational methods for fluid dynamics*. Berlin: Springer-Verlag; 1997.
5. Gibbons GH, Dzau VJ. 1994. The emerging concepts of vascular remodeling. *N. Engl. J. Med.* 330:1431-38
6. Guzman RJ, Abe K, Zarins CK. Flow-induced arterial enlargement is inhibited by suppression of nitric oxide synthase activity in vivo. *Surgery.* 1997 Aug;122(2):273-280. [PubMed]
7. Hassan T et al (2004) Computational replicas: anatomic reconstructions of cerebral vessels as volume numerical grids at three-dimensional angiography. *AJNR Am J Neuroradiol* 25 (8):1356-1365
8. Hassan T et al (2005) A proposed parent vessel geometry-based categorization of saccular intracranial aneurysms: computational flow dynamics analysis of the risk factors for lesion rupture. *J Neurosurg* 103(4):662-680
9. Lasheras J.C. The Biomechanics of Arterial Aneurysms, *Annu. Rev. Fluid Mech.* 2007. 39:293-319
10. Luscher, T. F. & Tanner, F. C. (1993). Endothelial regulation of vascular tone and growth. *American Journal of Hypertension* 6, 283-293S.
11. Malek A.M. and Izumo S. Mechanism of endothelial cell shape change and cytoskeletal remodeling in response to fluid shear stress. *Journal of Cell Science* 109, 713-726 (1996)
12. Valencia A, Zarate A, Galvez M, Non-Newtonian Badilla L. Blood flow dynamics in the internal carotid artery with a right saccular J-mutual aneurysm. *Int Methods Fluids* 2006, 50:751-64.)
13. Shojima M et al (2004) Magnitude and role of wall shear stress on cerebral aneurysm: computational fluid dynamic study of 20 middle cerebral artery aneurysms. *Stroke* 35(11):2500-2505